

Evaluation of multi-source satellite rainfall products in tekeze basin, Ethiopia

Masresha Ashenafi Kidie ¹, Achenafi Teklay ^{1*}

¹College of Agriculture and Environmental Science, Department of Natural Resource Management, University of Gondar.

*Corresponding author

Achenafi Teklay, University of Gondar, College of Agriculture and Environmental Sciences, Natural Resources Management, Gondar, Ethiopia, P. Box 196, Ethiopia

Email : achenafi.teklay@gmail.com

Received Date : April 16, 2024

Accepted Date : April 17, 2024

Published Date : May 17, 2024

ABSTRACT

Accurate and reliable rainfall information is crucial for regional water resource management, particularly in developing countries like Ethiopia. Unfortunately, Ethiopia faces challenges with sparse and inconsistent rainfall measurements, as well as a lack of updated data. As a result, the spatio-temporal characteristics of rainfall are poorly understood. In recent years, satellite-derived rainfall products have emerged as an alternative source of rainfall data to overcome these limitations. This study focuses on validating the performance of three satellite rainfall products, namely PERSIANN_CDR, CHIRPS, and TMPA3B42, over the Tekeze basin in Ethiopia. The evaluation involves assessing the prediction accuracy of these products using various statistical measures and spatial comparisons. The study period extends from 2007 to 2017. The results demonstrate that PERSIANN_CDR exhibits a very low percent bias (PBIAS), while CHIRPS and TMPA3B42 significantly overestimate observed rainfall. Moreover, PERSIANN_CDR performs well in capturing rainfall during the kiremt, belg, and bega seasons, with the lowest root mean square error (RMSE) values of 2.9, 1.4, and 0.8 mm/day, respectively. On the other hand, TMPA3B42 performs poorly during these seasons, showing the largest RMSE values of 3.1, 1.9, and 1.1 mm/day, respectively. In terms of detecting observed rainfall, both PERSIANN_CDR and TMPA3B42 exhibit good skills, while CHIRPS has the lowest detection skill across all seasons. Overall, the findings of this validation study

highlight the potential of the PERSIANN_CDR product for various operational applications in the Tekeze basin. It can be utilized for studying rainfall patterns and variability in the East African region.

Keywords : Satellite Rainfall Products, PERSIANN_CDR, CHIRPS, TMPA3B42, spatio-temporal, Tekeze basin

1. INTRODUCTION

Accurate and reliable information about rainfall is a crucial element in managing water resources on regional and global scales, and in regulating agricultural water use (Abro et al., 2021; Masood et al., 2023). Because rainfall affects the hydrological cycle and the earth's ecosystem, understanding its rate, amount, and distribution is imperative (Ahsan et al., 2023; Sreelash et al., 2018). Conventionally, rainfall data is derived from rain gauges, believed to be the most reliable method for measuring rainfall (Ayehu et al., 2018; Megersa et al., 2019; Qi, 2020). However, in developing countries, weather stations often face issues like sparse distribution, poor data quality, and lack of updated data, markedly in areas with inaccessible and rugged terrains, where rainfall variability is immense over short distances (Belete et al., 2020; Kimani et al., 2017; Zandler et al., 2019; Mekonen and Berlie, 2020; Ware et al., 2023). As a result, determining rainfall's spatial distribution over remote areas becomes highly complicated (Ayehu et al., 2018; Belay et al., 2019).

Over the years, satellite-derived rainfall estimates, with their long-term and spatially distributed nature, have emerged as a reliable source for overcoming these challenges (Feki et al., 2021; Girma and Berhanu, 2021; Alemayehu et al., 2020; Ayehu et al., 2018). Satellite Rainfall Products (SRPs) offer comprehensive data with fine temporal and spatial resolutions (Park et al., 2017). Therefore, evaluating their performance in different regions is essential for users, scientific communities, and algorithm developers (Belay et al., 2019). This evaluation helps in understanding and quantifying errors and uncertainties and recognizing the best SRPs for site-specific applications (Ayehu et al., 2018; Dinku et al., 2007; Jiang et al., 2016).

Several studies have been conducted to evaluate the performance of different satellite rainfall products (SRPs) in various regions of the world, including Asia (Ji et al., 2022; Kesarwani et al., 2023; Masood et al., 2023; Peng et al., 2021; Sharannya et al., 2020; Zhu et al., 2022), Africa (Gebrechorkos et al., 2020; Libanda et al., 2020; Omonge et al., 2022; Polong et

al., 2023), south America (Brasil Neto et al., 2021; dos Reis et al., 2017; Ringard et al., 2015) and europe (Aksu and Akgül, 2020; Zandler et al., 2019). These studies have shown that the performance of SRPs can vary significantly depending on the geographical location, topography, and season. For example, Xia et al. (2021) compared four SRPs with rain gauge data in the Pearl River Basin, China. They found that the satellite rainfall products generally performed well over the basin but showed limitations in detecting heavy rainfall events, underestimating high rainfall events, and overestimating the number of rainy days. Similarly, Musie et al. (2019) compared three SRPs over the Nile basin and recommended CHIRPS products due to their superior performance, potentially attributed to their fine spatial resolution. Previous researches still recommended to conduct site-specific validation of SRPs in diverse physiographic settings before using them for operational purposes.

Therefore, many SRP validation studies have been conducted in different parts of Ethiopia (Gebremicael et al., 2020, 2019; Reda et al., 2022; Seleshi and Zanke, 2004). However, these studies did not comprehensively validate the spatio-temporal rainfall variability derived from satellite rainfall estimates against observed rainfall values at the basin level. For instance, Seleshi and Zanke (2004) investigated the rainfall pattern in the upper part of the Tekeze basin using data from a single climatic station. Their findings indicated a consistent amount of rainfall over the past 40 years (1962–2002). Gebremicael et al. (2019) evaluated the performance of eight SRPs including TRMM, CHIRPS, RFEv2, ARC2, PERSIANN, GPCP, CMAP, and CMORPH in Upper Tekeze Atbar river basin. They compared these SRPs with varying spatial and temporal resolutions. The results indicated that CHIRPS consistently outperformed other products at all temporal and spatial scales. RFEv2, 3B42v7, and PERSIANN products also showed good agreement with gauge measurements for various spatio-temporal scales. Similarly, Reda et al. (2022) assessed the reliability of nine gridded precipitation datasets compared to ground-based observations in the Upper Tekeze River basin of Ethiopia. They evaluated precipitation at daily and monthly timescales. The findings revealed that the most accurate precipitation estimates were obtained from the Earth2Observe, WFDEI, and ERA-Interim reanalysis datasets.

Advancements in sensor technologies and estimation techniques have led to continuous improvements in the spatial and temporal resolutions as well as the measurement accuracy of SRPs. Notably, several higher resolution SRPs are now available on a quasi-global scale (Behrangi et al., 2011; Jiang et al., 2016). Out of the numerous options, three widely utilized precipitation datasets include Climate Hazards Group Infrared Rainfall with Stations (CHIRPS), Precipitation Estimation from Remotely Sensed Information Using Artificial

Neural Networks-Climate Data Record (PERSIANN_CDR), and The Tropical Rainfall Measurement Mission (TRMM) Multi-satellite Precipitation Analysis (TMPA). Therefore, this study was designed to assess the performance of these SRE products over the Tekeze basin. The research aims to answer two core questions: (1) What is the overall performance of each SRP? and (2) Which SRP performs best across various spatial and temporal timescales? For evaluation purposes, 45 rain gauges were utilized on a daily, monthly, and seasonal scale from 2007 to 2017. This study offers a comprehensive assessment across the Tekeze basin, considering a significant number of gauge stations, matching spatial and temporal resolutions to satellite products, and evaluating various aspects of performance. This research is followed novel approach by integrating various satellite rainfall products to assess their accuracy and reliability in a specific geographical location, the Tekeze Basin in Ethiopia. By comparing and evaluating the performance of these multi-source satellite rainfall datasets, the study offers insights into the practical implications of using such data for rainfall monitoring and forecasting in the region. This research contributes significantly to the field by addressing the critical need for comprehensive evaluations of satellite rainfall products, particularly in areas like the Tekeze Basin, to improve the understanding and utilization of satellite-based precipitation data for water resource management and disaster risk reduction purposes.

2. MATERIALS AND METHODS

2.1 Study area description

The Tekeze basin is situated in the North-western highlands of Ethiopia as part of the Upper Tekeze-Atbara River Basin, a significant tributary to the Nile River Basin. The total catchment area of the basin at the Wad El-Hilew outlet spans 66,543 km², encompassing regions of Ethiopia, Eritrea, and Sudan. Geographically, it is positioned between 36.1° E–39.5° E longitude and 11.4° N–14.5° N latitude (Figure 1). This area features rugged topography with notable elevation variance, ranging from 471 m above sea level (m.a.s.l) in the North-western part to 4540 m.a.s.l at Ras Dejen mountain.

The climate in the Tekeze basin displays semi-arid characteristics in the eastern and northern parts, transitioning to a partly sub-humid climate in the southern region, marked by a high seasonal rainfall pattern with substantial interannual variation (Conway, 2000). Annual mean rainfall varies from 400 mm/yr in the Northeast at Humera to over 1200 mm/yr in the Southwest near Ras Dejen mountain. The majority of the total annual precipitation, exceeding 85%, occurs during the wet (Kiremt) season, which extends from June to September. Rainfall patterns in the basin vary, displaying both monomodal characteristics in the western region and a bimodal (quasi-double maximum) pattern in the east, with peak rainfall

occurring in May and August. Ethiopia experiences three seasons, termed as Bega, Belg, and Kiremt. Bega refers to the dry season, spanning from October to January. Belg is a minor rainy season, reaching from February to May. Lastly, Kiremt is the primary rainy season that encompasses June to September.

Figure 1

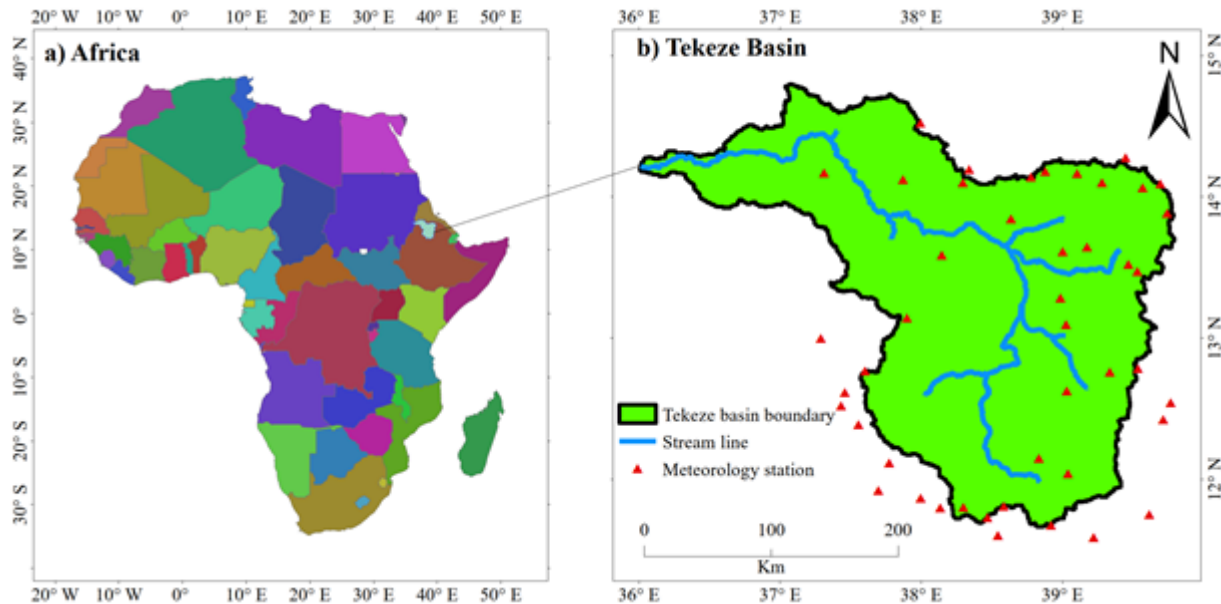


Figure 1. Study area; a) Africa regional map, and b) Upper Tekeze-Atbara River Basin (UTARB) with stream lines and Rainfall meteorology station.

2.2 Data collection

2.2.1 Observed rainfall data

Daily rainfall data for the Tekeze basin and surrounding areas was acquired from the National Meteorology Agency of Ethiopia (<http://www.ethiomet.gov.et>). This study utilized data from 45 meteorological stations across the 2007-2017 period to evaluate the performance of satellite-based rainfall products (Table 1).

Table 1. List of observed rainfall stations used for this study over the study area.

Id	Name	Lat.	Long.	Elev.	Id	Name	Lat.	Long.	Elev.
1	Abi_adi	13.61	39.00	1829	24	Gashena	11.68	38.92	2969
2	AddisZemen	12.12	37.77	1940	25	Gassay	11.80	38.13	2789
3	Adiawala	14.52	37.99	1570	26	Gondar	12.52	37.43	1973
4	Adigoshu	14.17	37.31	1114	27	Hagere Selam	13.65	39.17	2618
5	Adigrat	14.28	39.45	2497	28	Lalibela	12.04	39.04	2487
6	Adwa	14.18	38.88	1911	29	Maichew	12.78	39.53	2432
7	Ager genet	11.80	38.30	3010	30	Maksegnit	12.39	37.55	1912
8	Alamata	12.42	39.71	1589	31	MayTsebri	13.59	38.14	1349
9	Ambagiorgis	12.77	37.60	2900	32	MekeleAP	13.47	39.53	2257
10	Arb_Gebeya	11.60	38.54	2567	33	MekeleOB	13.52	39.47	2000
11	Atsebi	13.88	39.74	2711	34	Nebelet	14.10	39.28	1988
12	Axum_AP	14.14	38.78	2113	35	Nefasmewucha	11.73	38.47	3098
13	Aynbugna	12.15	38.83	2000	36	Sanja	12.99	37.29	1003
14	Chercher	12.54	39.77	1781	37	Sekota	12.63	39.03	2258

15	Debark	13.14	37.90	2836	38	Semema	14.19	38.34	1948
16	DebreZebit	11.81	38.58	3220	39	Senkata	14.06	39.57	2437
17	DebreTabor	11.87	37.99	2612	40	Shire	14.10	38.29	1897
18	EdagaSelus	13.84	38.63	2057	41	Sirinka	11.75	39.61	1861
19	Edagarbu	14.09	39.69	2920	42	Wedisemro	12.76	39.34	2456
20	Mayyohannes	14.12	37.87	1116	43	Wegel_Tena	11.59	39.22	2951
21	Feresmay	14.17	39.10	1948	44	Woreta	11.92	37.70	1819
22	Finarawa	13.10	39.02	1500	45	Yechila	13.28	38.98	1591
23	Dimma	13.68	38.32	1626					

2.2.2 Satellite rainfall products (SRPs)

In this study, the performance of three high-resolution satellite rainfall products (SRPs), namely the TRMM Multi-satellite Precipitation Analysis (TMPA) 3B42 algorithm (hereafter TMPA3B42), the Climate Hazards Group Infrared Precipitation Stations (CHIRPS), and the Precipitation Estimation from Remotely-Sensed Information using Artificial Neural Networks - Climate Data Record (PERSIANN_CDR), were evaluated (Table 2).

TMPA3B42 rainfall data

The TMPA3B42 version 7 was developed by the National Aeronautics and Space Administration NASA and the Japanese Aerospace Exploration Agency to monitor rainfall in tropical and subtropical regions (50° S – 50° N). This product provides daily rainfall data from 1998 to 2017 with a spatial resolution of 0.25° (<https://disc.gsfc.nasa.gov>).

CHIRPS rainfall data

The CHIRPS version 2 is a quasi-global (50° S - 50° N) and daily gridded product with a spatial resolution of 0.05° by 0.25° (Funk et al., 2015). It is designed for monitoring agricultural drought and global environmental change over land, and can also be used to simulate near-real-time initial hydrologic conditions. CHIRPS is a third-generation rainfall product that uses various interpolation schemes to create spatially continuous grids from raw point data (Ghozat et al., 2021).

Daily CHIRPS products at the spatial resolution of 0.25° are available from 1981 to the present (<ftp://chg-ftpout.geog.ucsb.edu/pub/org/chg/products/CHIRPS-2.0>).

Table 2. Summary of the satellite rainfall products used in this study.

SN	Rainfall products	Data input	Spatial resolution	Temporal resolution	Data source
1	TMPA3B42V7*	PMW + IR + satellite radar + gauge	0.25°	Daily	O & S
2	PERSIANN_CDR V1R1*	PMW (GPCP v2.2) + IR + gauge + ANN	0.25°	Daily	O & S
3	CHIRPSV2.0**	IR + TMPA3B42+gauge + CHPclim	0.25°	Daily	O, S, & R

Note: * Multi-satellite, **Infrared Estimate; O = Observed; S = Satellite; and R = Reanalysis.

PERSIANN_CDR rainfall data

The PERSIANN algorithm uses an artificial neural network (ANN) model to estimate precipitation using infrared (IR) data. The accuracy of PERSIANN is improved by adaptive adjustment of the network parameters using rainfall estimates from a passive microwave sensor. The PERSIANN_CDR product was developed by applying the PERSIANN algorithm to Gridded Satellite Infrared Data (GridSat-B1) and then bias-correcting estimations using monthly precipitation data (Ashouri et al., 2016). Daily PERSIANN_CDR product has been available for near-global coverage (60° S–60° N) with a spatial resolution of 0.25° since 1983 (<http://chrsdata.eng.uci.edu>).

2.3 Performance evaluation

The performance of three satellite-based rainfall products (SRPs) was evaluated using a range of statistical measures including

categorical, continuous, and spatial comparison methods.

2.3.1 Categorical validation statistics

To assess the rainfall estimation performance of the SRPs, a contingency table was constructed to evaluate the frequency of correct and incorrect estimated values (Table 3). The categorical statistical indices were then calculated to assess the SRPs' rain-detection capabilities. Four combinations between the estimated and observed data was used to verify the frequency of the correct and incorrect estimated values. These combinations are; a Hit (H) when a rainfall recorded by both satellite and rain gauge; Miss (M) when rain observed only by the rain gauge; False Alarm (F) when rain is recorded only by satellite; and Null (N) when no-rain recorded by both satellite and rain gauge. A threshold value of >1.0 mm/day was adopted to define whether there was rain or no rain event (Gao and Liu, 2013; Moazami et al., 2013).

Table 3. Contingency table between observed rainfall and SRPs estimation.

		Observed rainfall		
		Rain	No-rain	Total
Satellite Rainfall Products (SRPs)	Rain	Hit (H)	False Alarm (F)	H + F
	No-rain	Miss (M)	Null (N)	M + N
	Total	H + M	F + N	Total rainfall events (n)

These measures included categorical indices such as probability of detection (POD), false alarm ratio (FAR), and critical success index (CSI), as well as volumetric indices like volumetric miss ratio (MRV) and volumetric false ratio (FRV). POD measures the rain events that were correctly detected by the satellite (Equation 1); FAR measures the rain events that were incorrectly detected (Equation 2), and CSI is a measure of relative accuracy (Equation 3). The ideal value of POD and CSI is 1, whereas the best FAR value is 0 (Khan et al., 2023).

$$POD = H / (H + M) \quad (1)$$

$$FAR = F / (H + F) \quad (2)$$

$$CSI = H / (H + M + F) \quad (3)$$

Furthermore, the volumetric indices MRV (Equation 4) and FRV (Equation 5) were used to evaluate the products' volumetric performance. These indices range from 0 to 1, with 0 indicating the perfect estimation (Aghakouchak and Mehran, 2013).

$$MRV = \frac{\sum(O|(O > 1 \& S \leq 1))}{\sum(S|(S > 1 \& O > 1)) + \sum(O|(S \leq 1 \& O > 1))} \quad 4$$

$$FRV = \frac{\sum(S|(O \leq 1 \& S > 1))}{\sum(S|(S \geq 1 \& O > 1)) + \sum(O|(S \leq 1 \& O > 1))} \quad 5$$

Where H is the hit, M is the miss, F is the false alarm, O is the observed rainfall, and S is satellite rainfall estimation.

2.3.2 Continuous validation statistics

Additionally, continuous statistics such as correlation coefficient (CC), root mean square error (RMSE), and percent of bias (PBIAS) were used to evaluate the products' performance in estimating rainfall amount. The CC measures the degree of association between the observation and satellite estimations (Equation 6) values range from -1 to 1, representing a strong negative association and a strong positive association, respectively (Arellano et al., 2023). The RMSE measures the difference between observed and satellite rainfall (Equation 7), and the optimal value is 0 (Sadeghi et al., 2019). PBIAS measures the average difference between observation and satellite estimation (Equation 8), with positive values indicating overestimation bias and negative values indicating underestimation bias (Najmi et al., 2023). The optimal value of PBIAS is 0.

$$CC = \frac{\sum(S - Sav)(O - Oav)}{\sqrt{\sum(S - Sav)^2} \sqrt{\sum(O - Oav)^2}} \quad 6$$

$$RMSE = \sqrt{\frac{\sum(O - S)^2}{n}} \quad 7$$

$$PBIAS = \frac{\sum(S - O)}{\sum(O)} * 100 \quad 8$$

Where: O = the observed rainfall, Oav = the observed mean rainfall, S = the satellite rainfall product estimation, Sav = the mean satellite rainfall product, and n = the number of rainfall events. Besides, the cumulative distribution function (CDF) for the proportion of rainfall events, scatter plot, and Taylor diagram at daily, monthly, and seasonal time scales were used to evaluate the rainfall estimation performance of the three SRPs.

2.3.3 Spatial comparisons

To evaluate the spatial simulation performance of the SRPs, a comparison of the observed and estimated rainfall maps was conducted using the Kriging method. The advantages of Kriging include the estimation of an average value that takes account of the spatial correlation pattern of rainfall and the quantification of an error (Shitu et al., 2023; Workneh et al., 2024).

3.RESULTS

3.1 Temporal rainfall estimation

3.1.1 Daily rainfall

Table 4 shows the daily comparison between satellite rainfall products (SRPs) and a 0.25° aggregated rain gauge observation. Regarding the Percent Bias (PBIAS), the CHIRPS product had the highest value (22.8%), followed by TMPA3B42 (18.7%), overestimating the observed daily rainfall in the basin. Conversely, PERSIANN_CDR had the lowest PBIAS (5.2%), slightly overestimating the observed daily rainfall. All three satellite rainfall products (SRPs) had a strong correlation with observed daily rainfall, ranging from 0.80 to 0.82. PERSIANN_CDR had the highest correlation coefficient (CC) value among the SRPs. In terms of Root Mean Square Error (RMSE), PERSIANN_CDR had the lowest value (1.94 mm/day), while the CHIRPS rainfall product had the highest value (2.72 mm/day).

Table 4. Summary of statistical comparison between daily observation rainfall and SRPs estimation over the UTARB for the period 2007-2017. Note: the observed daily mean rainfall is 1.93 mm/day.

Satellite rainfall products	Mean (mm/day)	CC	RMSE (mm/day)	PBIAS (%)
PERSIANN_CDR	2.03	0.82	1.94	5.2
CHIRPS	2.37	0.81	2.72	22.8
TMPA3B42	2.29	0.80	2.15	18.7

The scatter plot of daily observed rainfall versus SRPs during the period 2007-2017 is shown in Figure 2. The PRSIANN_CDR product exhibited good accuracy in capturing the observed rainfall, while the TMPA3B42 product showed limited performance. All three SRPs tended to overestimate the observed rainfall, with the TMPA3B42 product showing a more pronounced overestimation in areas of maximum observed rainfall. The PRSIANN_CDR estimations had a relatively low deviation from the best fit values ($R^2 = 0.68$), whereas the TMPA3B42 estimations had the highest deviation ($R^2 = 0.64$).

Figure 2. Scatter plot of daily rainfall: observations (x-axis) versus SRPs estimations (y-axis).

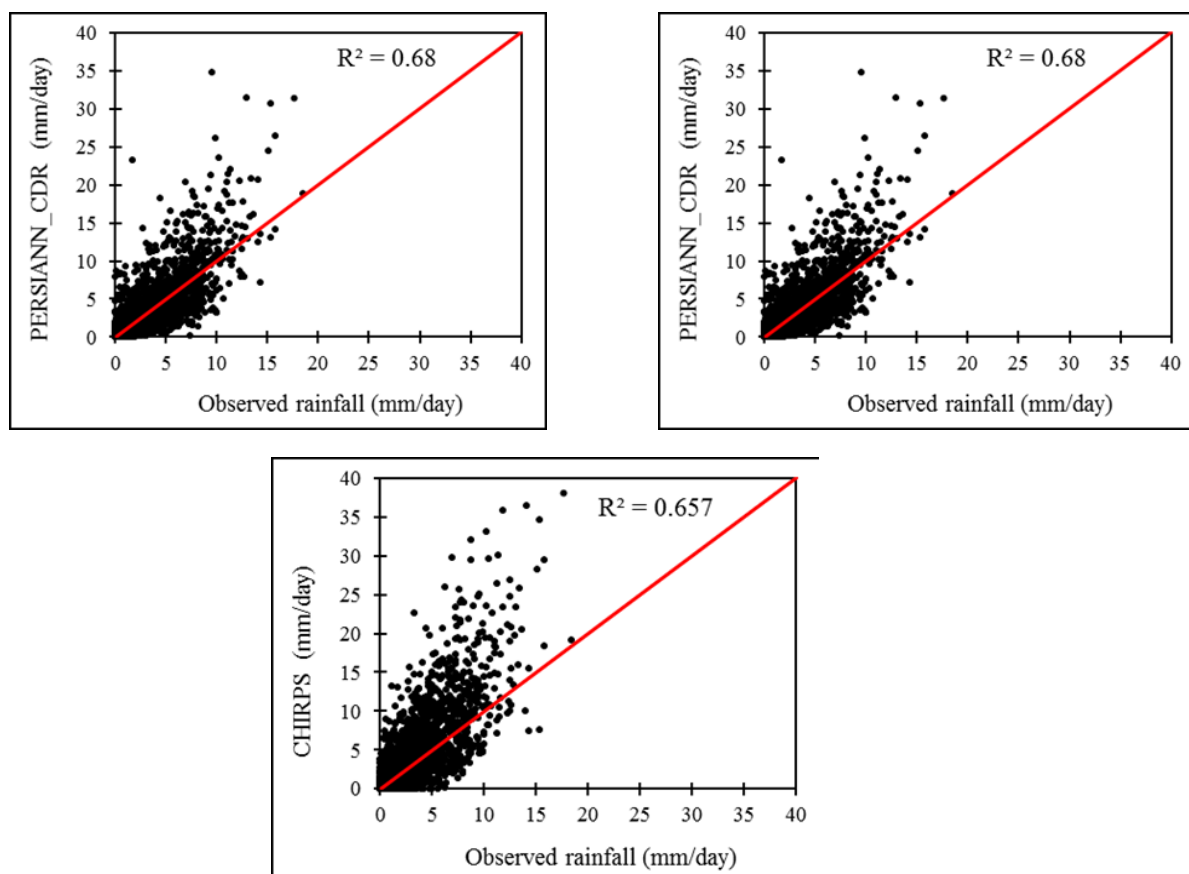


Figure 3 presents the Cumulative Distribution Function (CDF) of daily rainfall, comparing the SRPs with the observed data. Examining daily rainfall values from 2007 to 2017, the observed highest rainfall was 18.47 mm/day (Figure 3a). However, all three SRPs estimated significantly maximum rainfall values. The highest daily rainfall values from PERSIANN_CDR, TMPA3B42, and CHIRPS products were 34.81 mm/day, 38.51 mm/day, and 38.07 mm/day, respectively. At the 10% frequency level, both PERSIANN_CDR and TMPA3B42 estimations were slightly higher than the observed rainfall. In contrast, the CHIRPS estimations were significantly higher at this frequency. For instance, at the 5% frequency level, the observed rainfall was 7.7 mm (Figure 3a), while the estimations from PERSIANN_CDR and TMPA3B42 were 8.9 mm and 9.6 mm, respectively. The CHIRPS estimation was 11.3 mm, showing a larger deviation from the observed rainfall at this frequency. Furthermore, the PERSIANN_CDR estimations closely matched the observed rainfall at most frequency levels. In Figure 4b, it can be observed that the number of rainfalls below 5 mm/day accounted for 12.75% and 13.3% of the observed and PERSIANN_CDR data, respectively. However, this class represented 16.3% and 17.5% of the CHIRPS and TMPA3B42 data, respectively. This indicates that the PERSIANN_CDR estimation aligned closely with the observed values in the daily time series.

Figure 3

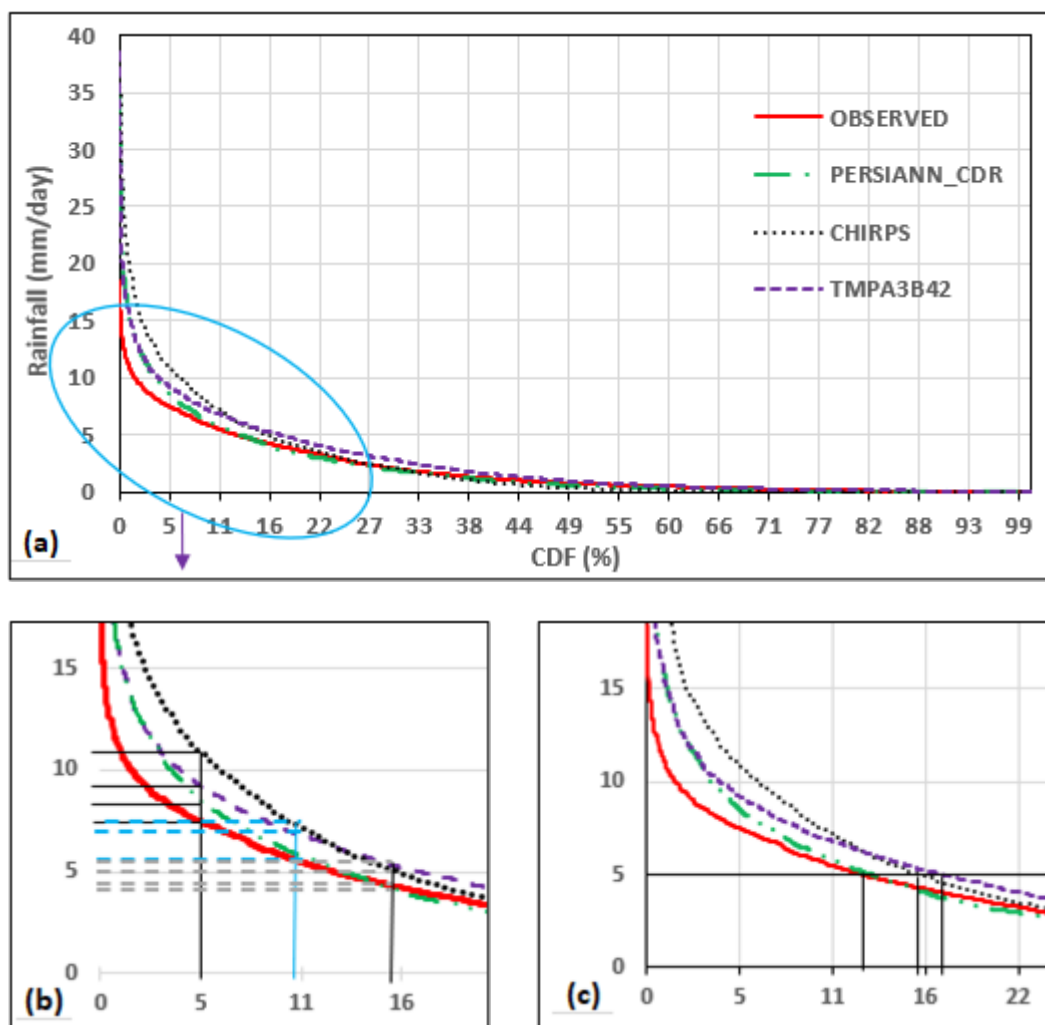


Figure 3. (a) Cumulative distribution function (CDF) of daily rainfall for rain gauge and the three SRPs over the UTARB for a period 2007-2017, b) rainfall at 5, 10, & 15% of frequency, and c) different frequencies at 5 mm of rainfall.

All three SRP estimations demonstrated a strong association with the observed rainfall. Both PERSIANN_CDR and TMPA3B42 closely matched the observed daily mean rainfall, exhibiting a slightly lower Root Mean Square Error (RMSE) and a higher correlation (**Figure 4a**). The spatial variability in all SRP estimations exceeded that of the observed rainfall (2.6 mm/day). Notably, the CHIRPS product had considerably higher spatial variation compared to the observed rainfall. Overall, the PERSIANN_CDR product performed well in estimating the observed rainfall, as it had the lowest RMSE (1.94 mm/day) and spatial variability (3.5 mm/day), along with the highest correlation (0.83). Conversely, the CHIRPS product performed poorly, with the highest RMSE (2.7 mm/day) and spatial variation (4.3 mm/day), and the lowest pattern correlation (0.8).

Figure 4

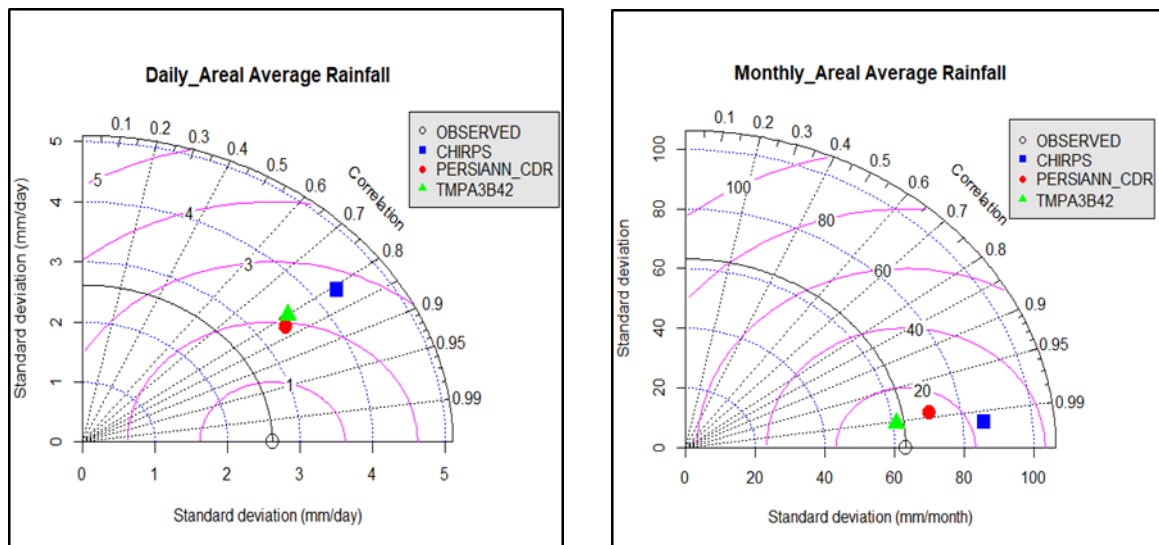


Figure 4. Taylor diagram showing a statistical comparison between SRPs and observed rainfall at; a) Daily, and b) Monthly areal average.

3.1.2 Monthly rainfall

The monthly rainfall analysis was conducted by adding up the daily rainfall data from 2007 to 2017. The analysis revealed that all three SRPs were highly correlated with the observed monthly rainfall, with correlation coefficients ranging from 0.94 to 0.96 (Table 5). This indicates a significant improvement compared to the daily time scales where the correlation coefficients were 0.80 to 0.82 (Table 4). Among the SRPs, the PERSIANN_CDR product exhibited the lowest Root Mean Square Error (RMSE) of 22.7 mm/month and Percent Bias (PBIAS) of 5.3%, indicating better accuracy. On the other hand, the CHIRPS product had the highest RMSE of 36.5 mm/month and PBIAS of 23% (Table 5). In general, the PERSIANN_CDR product demonstrated better performance in estimating monthly rainfall, closely resembling the observed rainfall.

Table 5. Summary of statistical comparison between monthly observation rainfall and SRPs estimation over the UTARB for the period 2007-2017. Note: the observed mean monthly rainfall is 56.65 mm/month.

Satellite rainfall products	Mean (mm/month)	CC	RMSE (mm/month)	PBIAS (%)
PERSIANN_CDR	61.8	0.96	22.7	5.3
CHIRPS	72.1	0.95	36.5	23
TMPA3B42	69.7	0.94	28.6	18.8

Figure 5 illustrates the mean monthly rainfall observed and estimated by the SRPs for the period of 2007-2017. Among the SRPs, the CHIRPS product reported the highest and lowest average monthly rainfall in August (264.6 mm/month) and December (4.2 mm/month) respectively. All of the SRPs tended to overestimate the observed rainfall during the wet months of July and August, as well as the dry months of October and November. However, they underestimated the observed rainfall in February and March. The CHIRPS product had the highest overestimation, reaching 68 mm/month in July. Overall, the PERSIANN_CDR product accurately estimated the observed rainfall in most months, except for May, June, and August (as depicted in Figure 5).

Figure 5

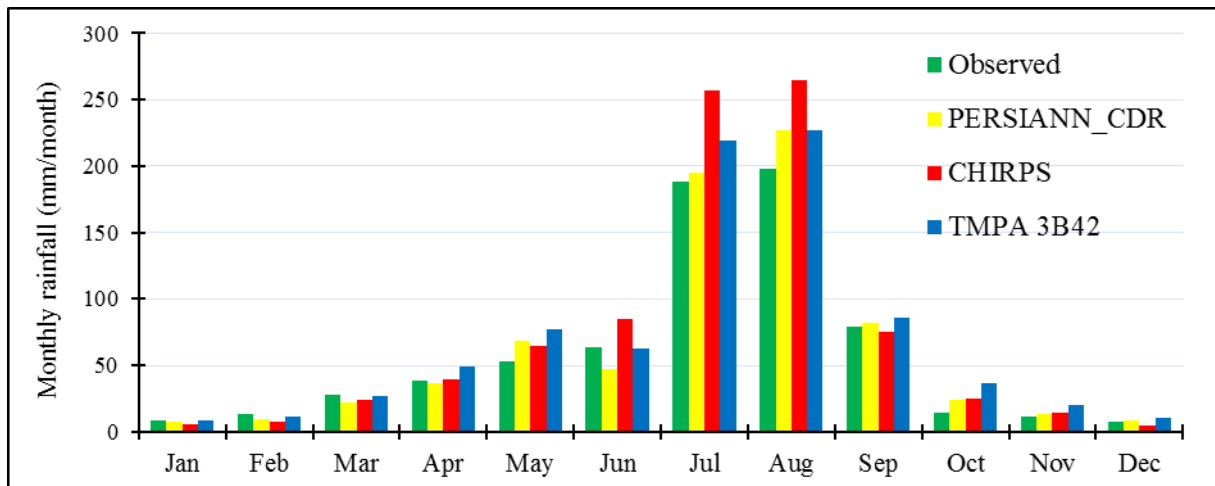


Figure 5. Long term monthly areal mean rainfall (2007-2017) from observed and SRPs.

3.1.3 Seasonal rainfall

Table 6 presents a seasonal comparison of observed and SRP rainfall estimations. During the Belg season (semi-dry season = February to May), both the PERSIANN_CDR and CHIRPS products exhibited a strong association with the observed rainfall (Table 6). The PERSIANN_CDR product demonstrated the lowest RMSE value of 1.39 mm/day, while the TMPA3B42 product had the highest RMSE value of 1.86 mm/day during this season. Although both the PERSIANN_CDR and CHIRPS products slightly overestimated the Belg season rainfall, the TMPA3B42 product significantly overestimated it by 24.7%. In the Kiremt season (wet season = June to September), all three SRPs showed a very good correlation with the observed rainfall, with the highest correlation coefficient (CC) found in the PERSIANN_CDR product (0.76). The PERSIANN_CDR product also had the lowest RMSE value of 2.94 mm/day compared to the other products. However, all three SRPs overestimated the observed rainfall during the Kiremt season. The PERSIANN_CDR product had the lowest overestimation (4.2%), while the CHIRPS product had the highest overestimation (28.6%). In the Bega season, the correlation between observed and estimated rainfall from the three products was poor (Table 6). The PERSIANN_CDR product had the lowest error variance of 0.8 mm/day, while the TMPA3B42 product had the highest RMSE value of 1.06 mm/day during this season. The CHIRPS product had the lowest PBIAS of 17.9%, indicating a slight overestimation of the observed rainfall. However, the TMPA3B42 product significantly overestimated the observed rainfall, with a PBIAS value of 80.8%. Overall, the PERSIANN_CDR product accurately represented the observed rainfall in all three seasons.

Table 6. Summary of statistical comparison between seasonal observation rainfall and SRPs estimation over the UTARB for the period 2007-2017.

Season	Statistical measures	Observed rainfall	Satellite Rainfall Products (SRPs)		
			PERSIANN-CDR	CHIRPS	TMPA3B42
Belg	Mean (mm/day)	1.10	1.14	1.12	1.38
	CC	-	0.69	0.68	0.60
	RMSE (mm/day)	-	1.39	1.70	1.86
	PBIAS (%)	-	3.1	2.0	24.7
Kiremt	Mean (mm/day)	4.34	4.52	5.58	4.88
	CC	-	0.76	0.73	0.74
	RMSE (mm/day)	-	2.94	4.30	3.05
	PBIAS (%)	-	4.2	28.6	12.5
Bega	Mean (mm/day)	0.34	0.43	0.40	0.61
	CC	-	0.63	0.59	0.59
	RMSE (mm/day)	-	0.80	0.90	1.06
	PBIAS (%)	-	27.4	17.9	80.8

3.2 Spatial rainfall estimation

The spatial comparison of mean bias on different temporal scales is presented in Figures 6-9. The analysis of mean annual results revealed that the SRPs exhibited both overestimation and underestimation of rainfall across the basin (Figure 6). Specifically, the TMPA3B42 and PERSIANN_CDR products slightly underestimated rainfall in the southern and northern regions of the basin, while they slightly overestimated it in the western and central areas. On the other hand, the CHIRPS product significantly overestimated rainfall in most parts of the basin, with the highest overestimation (80-100 mm/year) observed in the western region

Figure 6

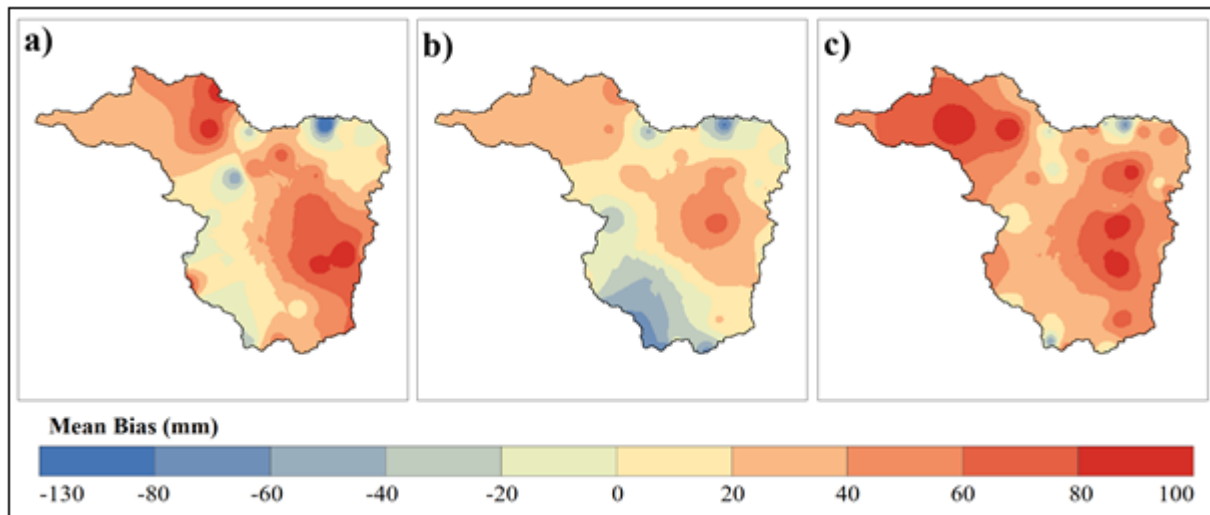


Figure 6. Spatial distribution of mean annual bias (SRPs-Observed) over UTARB; a) TMPA3B42; b) PERSIANN_CDR; and c) CHIRPS.

During the Belg season, the TMPA3B42 product demonstrated a favorable tendency in estimating observed rainfall, with a mean bias ranging from -30 to 15 mm across the entire basin (Figure 7a). The PERSIANN_CDR product accurately reproduced observed rainfall in the northern and southern regions of the basin, but it overestimated rainfall in the western and central areas (Figure 7b). Conversely, the CHIRPS product exhibited substantial overestimation (60 mm) in the central part of the basin, while underestimating rainfall (60 to 75 mm) in the northern and southern tips (Figure 7c).

Figure 7

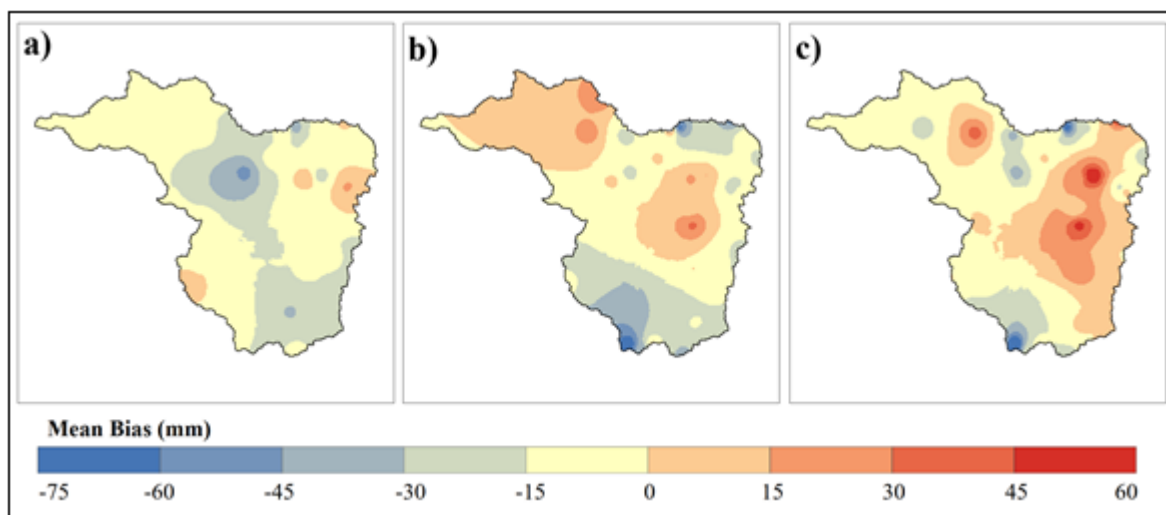


Figure 7. Spatial distribution of Belg season mean bias (SRPs-Observed) over UTARB; a) TMPA3B42; b) PERSIANN_CDR; and c) CHIRPS.

During the Kiremt seasons, the TMPA3B42 product performed well in estimating observed rainfall in the southwestern and western parts of the basin, but demonstrated considerable tendencies of overestimation and underestimation in the eastern and southern regions, respectively (Figure 8a). The PERSIANN_CDR product provided a reliable estimation of observed rainfall across most parts of the basin, except for a slight overestimation in the eastern part and an underestimation in the southwestern regions (Figure 8b). On the other hand, the CHIRPS product significantly overestimated rainfall throughout the entire basin, with the highest overestimation of 120 mm observed in the western part (Figure 8c).

Figure 8

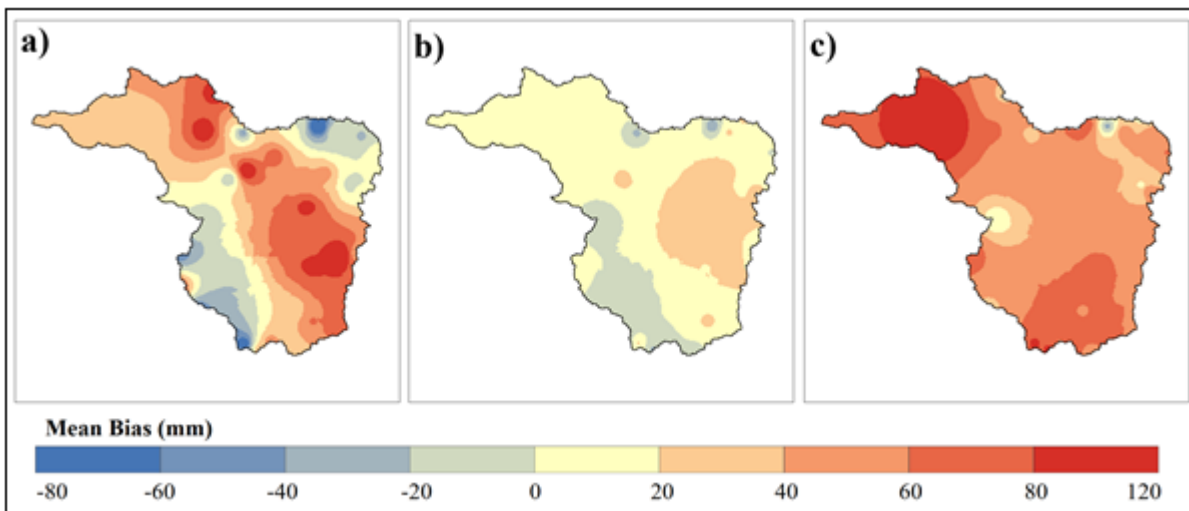


Figure 8. Spatial distribution of Kiremt season mean bias (SRPs-Observed) over UTARB; a) TMPA3B42; b) PERSIANN_CDR; and c) CHIRPS.

During the bega season, the CHIRPS product accurately reproduced the spatial pattern of observed rainfall across all parts of the basin (Figure 9c). It slightly overestimated rainfall (10 mm) in the central area, while slightly underestimating it (10 mm) in the southern and western regions. The PERSIANN_CDR product exhibited a good pattern in the northern and southern parts of the basin, but overestimated rainfall in the central and western areas (Figure 9b). However, the TMPA3B42 product performed poorly in most parts, mainly due to a significant overestimation of observed rainfall (Figure 9a).

Figure 9

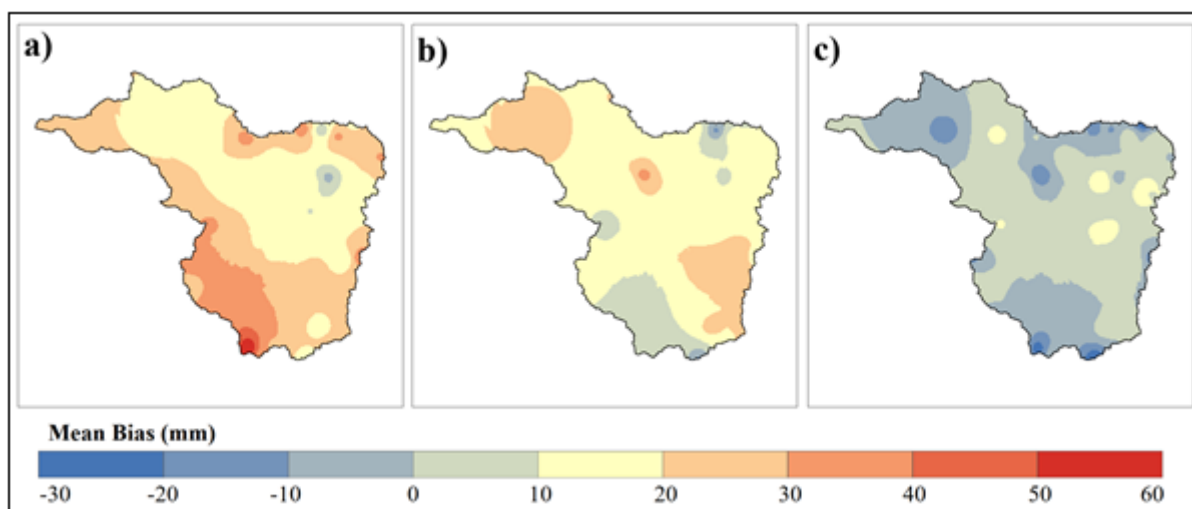


Figure 9. Spatial distribution of Bega season mean bias (SRPs-Observed) over UTARB; a) TMPA3B42; b) PERSIANN_CDR; and c) CHIRPS.

3.3 Rainfall detection

3.3.1 Rainfall event detection

The three SRPs demonstrated good detection of observed rainfall events, with POD values exceeding 0.7 (Figure 10). The

TMPA3B42 product achieved the highest POD of 0.81, while CHIRPS had the lowest POD of 0.70. The superior potential for rainfall detection in TMPA3B42 may be attributed to its retrieval algorithm. Additionally, all SRPs exhibited very high CSI values ranging from 0.64 to 0.73, indicating that more than 64% of observed rainfall events were accurately detected by the SRPs. However, it is worth noting that some observed rainfall events were missed by the SRP estimations. Among the SRPs, PERSIANN_CDR had the lowest FAR value of 0.10, while TMPA3B42 had the highest FAR value of 0.15. This indicates that approximately 15% of the estimated rainfall by TMPA3B42 was not observed, emphasizing the importance of considering such discrepancies.

Figure 10

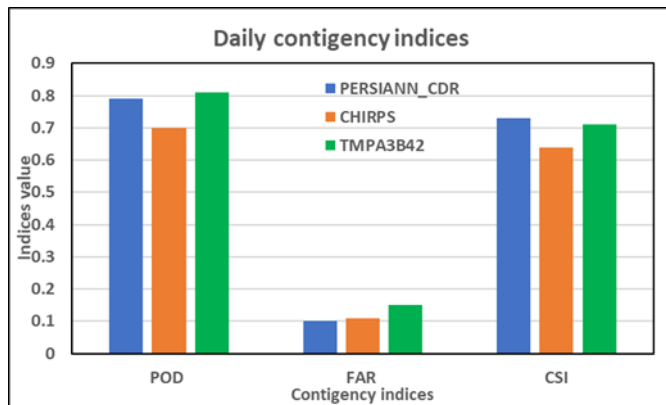
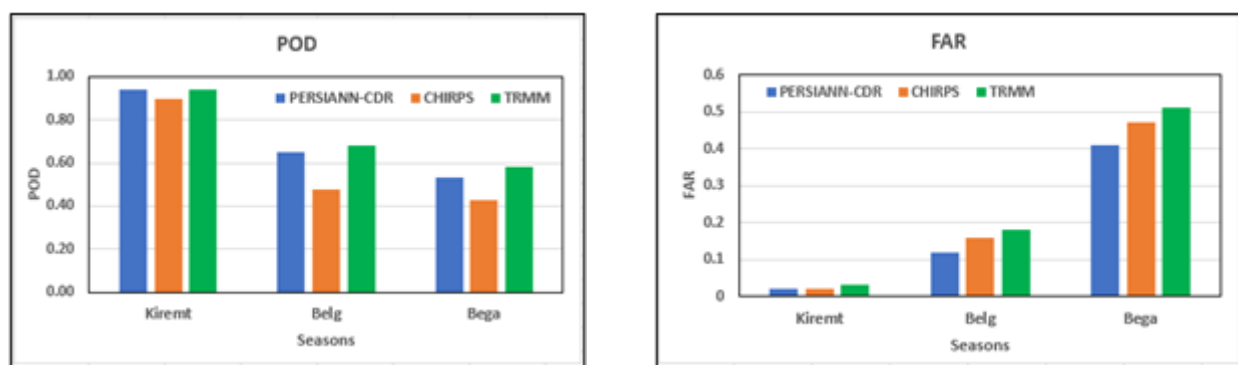


Figure 10. Summary of daily contingency indices (rainfall detection) comparison of satellite rainfall products with observed rainfall over the UTARB for the period 2007-2017.

As depicted in Figure 11, the three products demonstrated their highest detection skill during the Kiremt season, with POD values exceeding 90%, CSI values surpassing 88%, and FAR values below 3%. However, their performance was comparatively poor in detecting rainfall during the Bega season, with POD values below 58%, CSI values below 36%, and FAR values exceeding 41%. In the Kiremt season, PERSIANN_CDR and TMPA3B42 products correctly detected 94% of observed rainfall events, exhibiting the highest performance. Conversely, during the Bega season, SRPs detected less than 58% of observed rainfall events, with CHIRPS correctly detecting only 45% of rainfall in this season. In terms of overall skill in detecting the rainy season, all rainfall products displayed similar performance, with FAR values below 3%. However, SRPs falsely detected observed rainfall events by over 41% during the Bega season, with the highest value of 51% observed in the TMPA3B42 product. The CSI values indicated that during the Kiremt season, both PERSIANN_CDR and TMPA3B42 products exhibited an equivalent CSI value of 92% for correctly detecting rainfall events, followed by CHIRPS with an 88% CSI value. In the Bega season, PERSIANN_CDR exhibited the highest CSI value of 39%, followed by TMPA3B42 with 36% and CHIRPS with 33%.

Figure 11



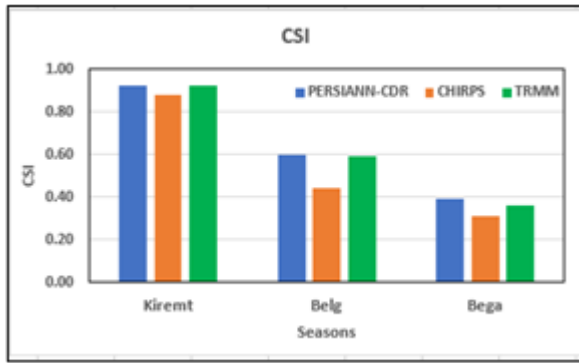


Figure 11. Comparisons of categorical indices (POD, FAR, & CSI) for Kiremt, Belg, and Bega seasons over UTARB from a period 2007-2017.

The comparison between observed and SRP frequency detection for different rainfall classes is shown in Figure 12. All three SRPs exhibited a slight underestimation of the number of observed rainfall events smaller than 5 mm. However, the TMPA3B42 product slightly overestimated the observed rainfall events between 5 mm and 10 mm, while the PERSIANN_CDR and CHIRPS products slightly underestimated the observed rainfall events in the same range. For rainfall events between 10 mm and 50 mm, all SRPs overestimated the number of observed events, with the CHIRPS product showing the highest overestimation (Figure 12). Both PERSIANN_CDR and TMPA3B42 had equal frequencies in rainfall events ranging from 15–25 mm (heavy rain) and 25–50 mm (very heavy rainfall). In general, the PERSIANN_CDR product displayed a closer number of frequencies to the observed rainfall in most classes, indicating a relatively better alignment with the actual rainfall observations.

Figure 12

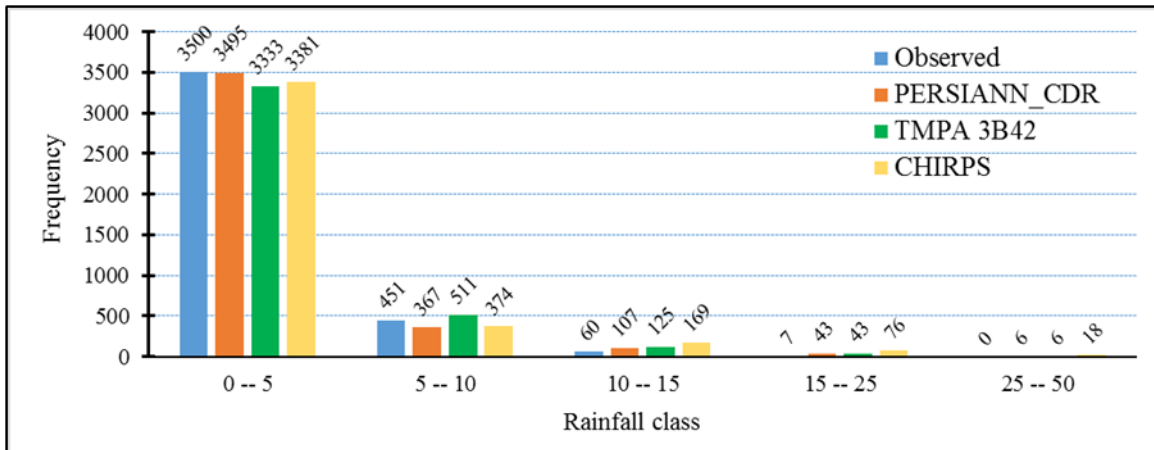


Figure 12. Comparisons of rainfall events at different classes between observed and SRPs.

3.3.2 Rainfall volume detection

Table 7 presents the missed and false rainfall volume detection of the three SRPs across daily and seasonal time scales. The estimated missed rainfall volume (MRV) showed insignificant variation among the three SRPs for both daily and seasonal time scales. However, the estimated false rainfall volume (FRV) exhibited significant variation across all time scales, except for the kiremt season. In terms of daily rainfall, CHIRPS product had a slightly lower MRV value of 1.1% (Table 7). Conversely, the PERSIANN_CDR and TMPA3B42 products demonstrated a low FRV value of 3.3% for daily rainfall.

Table 7. Comparisons of rainfall volume detection from daily and seasonal time scales.

Satellite Rainfall Products	MRV (%)				FRV (%)			
	Annual	Kiremt	Belg	Bega	Annual	Kiremt	Belg	Bega
PERSIANN_CDR	1.2	0.38	3.6	4.2	3.3	0.52*	6.4	28.4
CHIRPS	1.1	0.38	3.8	5.3	7.8	0.57	5.9	29.3
TMPA3B42	1.3	0.34	3.6	4.4	3.3	0.67	10.8	50.2

Note: MRV= miss rainfall volume, FRV= false rainfall volume.

During the Kiremt season, all SRPs exhibited lower MRV values ranging from 0.34% to 0.38%. In the Belg season, both PERSIANN_CDR and TMPA3B42 had equivalent MRV values of 3.6%, while CHIRPS had a slightly higher MRV of 3.8%. Moving to the Bega season, PERSIANN_CDR products had the lowest MRV value of 4.2%, while CHIRPS had the highest MRV value of 5.3%. During the Bega season, TMPA3B42 had a higher FRV value of 50.2% compared to CHIRPS (29.3%) and PERSIANN_CDR (28.4%). In the Belg season, TMPA3B42 also had a higher FRV value of 10.8% compared to PERSIANN_CDR (6.4%) and CHIRPS (5.9%). Additionally, during the Kiremt season, TMPA3B42 had a slightly higher FRV value of 0.67% compared to CHIRPS (0.57%) and PERSIANN_CDR (0.52%).

4. DISCUSSIONS

The PERSIANN_CDR product slightly overestimated observed rainfall with a lower PBIAS value of 5.3%. In contrast, CHIRPS and TMPA3B42 products significantly overestimated observed rainfall by 23% and 18.8%, respectively. The poor performance of these satellite-derived products at the daily time scale can be attributed to high rainfall variability in topographically complex areas, and the scale difference between satellite-derived rainfall products and in-situ observations (Rahmawati and Lubczynski, 2018). However, the association between SRPs and observed monthly rainfall improved significantly compared to the daily timescale. The PERSIANN_CDR had a strong association with the observed monthly rainfalls. This finding aligns with Zambrano-bigiarini et al. (2017), indicating that satellite products perform better at higher temporal aggregation.

During the Belg season, both PERSIANN_CDR and CHIRPS exhibited lower overestimation of observed rainfall with PBIAS values of 3.1% and 2.0% respectively. However, during the bega season, both products showed higher overestimation, while PERSIANN_CDR estimated lower overestimation during the kiremt season. This suggests that injecting gauge observations into the model improves the performance of SRPs. The overestimation of CHIRPS in the Kiremt season can be attributed to the TIR sensor's limitation in distinguishing cirrus clouds from rain clouds (Dinku et al., 2014; Thiemig et al., 2012; Young et al., 2014). It is important to validate and

bias correct satellite-derived products before using them in hydrological studies, as regional and local factors can influence their performance (Zambrano-bigiarini et al., 2017; Fenta et al., 2018).

In the Bega season, CHIRPS had a lower PBIAS value of 17.9% compared to PERSIANN_CDR (27.4%) and TMPA3B42 (80.8%). This finding is consistent with previous studies by Guerhazi et al. (2019), Sinta et al. (2022), Tadesse et al. (2022), and Polong et al. (2023). CHIRPS also exhibited too few dry days, attributed to the use of TMPA3B42 for establishing regression equations linking infrared-based cold-cloud duration values to 5-day mean rainfall (Funk et al., 2015). Reanalyses consistently underestimated the number of dry days globally due to deficiencies in representing and parameterizing the physical processes governing rainfall generation (Hua et al., 2019; Jafarpour et al., 2022; Miao et al., 2021; Wanzala et al., 2022; Zhang et al., 2021). The higher PBIAS during the Bega season in PERSIANN_CDR may be related to higher evaporation of rainfall before reaching the land surface, leading to overestimation of rainfall from rain gauges by satellite rainfall products.

Overall, the three satellite rainfall products generally represented observed rainfall well in all seasons. PERSIANN_CDR had a good correlation with observed rainfall in all seasons, while TMPA3B42 had a higher Percent of Detection (POD) for observed rainfall values compared to the other products. The overestimation of rainy days by CHIRPS may be attributed to the process of translating infrared CCD values into precipitation estimates using the 0.25° grid cell TMPA datasets, which can result in an excessive amount of light rain (Funk et al., 2015). These findings highlight significant discrepancies in the quality of available rainfall products across daily to monthly time scales. Spatial-temporal assessment in this study allowed for identifying sources of errors, such as the effect of various sensors, topography, and retrieval algorithms (Beighley et al., 2011; Liu et al., 2022; Qin et al., 2014).

5. CONCLUSIONS AND RECOMMENDATIONS

In summary, this study extensively assessed the suitability and dependability of satellite rainfall products (PERSIANN_

CDR, CHIRPS, and TMPA3B42) in the Tekeze basin from 2007 to 2017. The analysis revealed that CHIRPS exhibited a higher positive bias in daily timescales compared to TMPA3B42, while PERSIANN_CDR displayed a considerably low positive bias in daily timescales.

The comparative analysis further indicated that PERSIANN_CDR outperformed CHIRPS and TMPA3B42 in terms of continuous statistical error metrics (CC, RMSE, and PBIAS) across daily, monthly, and seasonal time scales. Additionally, PERSIANN_CDR demonstrated excellent accuracy in detecting rainfall events (POD, FAR, and CSI) and volume (MRV and FRV) on daily and seasonal scales. These findings highlight the potential of the PERSIANN_CDR product for various operational applications, including the study of spatiotemporal rainfall patterns and variability in the complex topography of the Tekeze basin in Ethiopia.

This validation study serves as a valuable reference for future applications of satellite rainfall estimates in hydrological modeling, particularly in basins with limited rain gauges and rugged terrain, like the Tekeze basin. We recommend conducting further studies to gain a comprehensive understanding of the accuracy of satellite rainfall estimates, such as assessing hydrological evaluation through streamflow simulation using different models (e.g., SWAT, HBV-light, HEC-HMS). Additionally, it would be beneficial to evaluate the impacts of various bias correction methods on model simulations in the basin.

In future studies, it is essential to prioritize the improvement of ground truth data availability and accuracy, as this will positively impact the robustness and reliability of the evaluation process. Additionally, the inclusion of diverse geographical areas beyond the Tekeze Basin in Ethiopia would contribute to enhancing the generalizability of findings, enabling a better understanding of how different regions or basins respond to similar methodologies. A more extensive time frame should be considered to capture long-term rainfall trends and seasonal variations, providing a more comprehensive view of the performance of satellite rainfall products. It is crucial for future studies to account for external factors such as climate change, land use changes, and anthropogenic influences, in order to offer a more comprehensive analysis of the satellite rainfall products' performance under varying conditions. Furthermore, addressing the limitations associated with each satellite rainfall product, including spatial resolution, retrieval algorithms, and calibration issues, is paramount to achieving more accurate and reliable evaluations. Embracing technological advancements, such as improved satellite sensors and data processing techniques, can significantly enhance the accuracy and efficiency of satellite rainfall estimation, particularly in complex terrains like the Tekeze Basin. Collaboration with experts from various fields like meteorology, remote sensing, and hydrology would bring

valuable insights and perspectives to the methodology, ensuring a more comprehensive and robust evaluation process. By integrating these recommendations into future studies, researchers can elevate the methodology employed in evaluating multi-source satellite rainfall products, leading to more accurate and insightful findings.

Acknowledgments

The authors acknowledge the National Meteorological Service Agency of Ethiopia (NMSA) for providing rainfall data (<http://www.ethiomet.gov.et>).

REFERENCES

1. Abro, M.I., Zhu, D., Elahi, E., Majidano, A.A., Solangi, B.K., 2021. Hydrological simulation using multi-sources precipitation estimates in the Huaihe River Basin.
2. Aghakouchak, A., Mehran, A., 2013. Extended contingency table: Performance metrics for satellite observations and climate model simulations. *Water Resour. Res.* 49, 7144–7149. <https://doi.org/10.1002/wrcr.20498>
3. Ahsan, S., Bhat, M.S., Alam, A., Sheikh, H.A., Farooq, H., 2023. Hydrological extremes and climatic controls on streamflow in Jhelum basin, NW Himalaya. *Theor. Appl. Climatol.* 151, 1729–1752. <https://doi.org/10.1007/s00704-022-04346-4>
4. Alemayehu, A., Maru, M., Bewket, W., Assen, M., 2020. Spatiotemporal variability and trends in rainfall and temperature in Alwero watershed, western Ethiopia. *Environ. Syst. Res.* 9. <https://doi.org/10.1186/s40068-020-00184-3>
5. Ashouri, H., Hguyen, P., Thorstensen, A., Hsu, K., Sorooshian, S., Braithwaite, D., 2016. Assessing the Efficacy of High-Resolution Satellite-Based PERSIANN-CDR Precipitation Product in Simulating Streamflow. *J. Hydrometeorol.* 17, 2061–2076. <https://doi.org/10.1175/JHM-D-15-0192.1>
6. Ayehu, G.T., Tadesse, T., Gessesse, B., Dinku, T., 2018. Validation of new satellite rainfall products over the Upper Blue Nile Basin, Ethiopia 1921–1936.
7. Behrangi, A., Khakbaz, B., Chun, T., Aghakouchak, A., Hsu, K., 2011. Hydrologic evaluation of satellite precipitation products over a mid-size basin. *J. Hydrol.* 397, 225–237. <https://doi.org/10.1016/j.jhydrol.2010.11.043>

8. Beighley, R.E., Ray, R.L., He, Y., Lee, H., Schaller, L., Andreadis, K.M., Durand, M., Alsdorf, D.E., Shum, C.K., 2011. Comparing satellite derived precipitation datasets using the Hillslope River Routing (HRR) model in the Congo River Basin. *Hydrol. Process.* 25, 3216–3229. <https://doi.org/10.1002/hyp.8045>
9. Belay, A.S., Fenta, A.A., Yenehun, A., Nigate, F., Tilahun, S.A., Moges, M.M., Dessie, M., Adgo, E., Nyssen, J., Chen, M., Van Griensven, A., Walraevens, K., 2019. Evaluation and application of multi-source satellite rainfall product CHIRPS to assess spatio-temporal rainfall variability on data-sparse western margins of Ethiopian highlands. *Remote Sens.* 11, 1–22. <https://doi.org/10.3390/rs11222688>
10. Belete, M., Deng, J., Wang, K., Zhou, M., Zhu, E., Shifaw, E., Bayissa, Y., 2020. Evaluation of satellite rainfall products for modeling water yield over the source region of Blue Nile Basin. *Sci. Total Environ.* 708, 134834. <https://doi.org/10.1016/j.scitotenv.2019.134834>
11. Conway, D., 2000. The climate and hydrology of the Upper Blue Nile river. *Geogr. J.* 166, 49–62. <https://doi.org/10.1111/j.1475-4959.2000.tb00006.x>
12. Dinku, T., Ceccato, P., Connor, S.J., 2007. Validation of Satellite Rainfall Products over East Africa ' s Complex International Journal of Remote Validation of satellite rainfall products over East Africa ' s complex topography. <https://doi.org/10.1080/01431160600954688>
13. Dinku, T., Hailemariam, K., Maidment, R., Tarnavskyc, E., Connor, S., 2014. Combined use of satellite estimates and rain gauge observations to generate high- quality historical rainfall time series over Ethiopia. *Int. J. Climatol.*
14. Feke, B.E., Terefe, T., Ture, K., Hunde, D., 2021. Spatiotemporal variability and time series trends of rainfall over northwestern parts of Ethiopia: the case of Horro Guduru Wollega Zone. *Environ. Monit. Assess.* 193. <https://doi.org/10.1007/s10661-021-09141-8>
15. Fenta, A.A., Yasuda, H., Shimizu, K., Ibaraki, Y., Haregeweyn, N., Kawai, T., Belay, A.S., Sultan, D., Ebabu, K., 2018. Evaluation of satellite rainfall estimates over the Lake Tana basin at the source region of the Blue Nile River. *Atmos. Res.* 212, 43–53. <https://doi.org/10.1016/j.atmosres.2018.05.009>
16. Funk, C., Peterson, P., Landsfeld, M., Pedreros, D., Verdin, J., Shukla, S., Husak, G., Rowland, J., Harrison, L., Hoell, A., Michaelsen, J., 2015. The climate hazards infrared precipitation with stations — a new environmental record for monitoring extremes 1–21. <https://doi.org/10.1038/sdata.2015.66>
17. Gao, Y.C., Liu, M.F., 2013. Evaluation of high-resolution satellite precipitation products using rain gauge observations over the Tibetan Plateau. *Hydrol. Earth Syst. Sci.* 17, 837–849. <https://doi.org/10.5194/hess-17-837-2013>
18. Ghozat, A., Sharafati, A., Hosseini, S.A., 2021. Long-term spatiotemporal evaluation of CHIRPS satellite precipitation product over different climatic regions of Iran. *Theor. Appl. Climatol.* 143, 211–225. <https://doi.org/10.1007/s00704-020-03428-5>
19. Girma, D., Berhanu, B., 2021. Evaluation of the Performance of High-Resolution Satellite Based Rainfall Products for Stream Flow Simulation. *J. Civ. Environ. Eng.* ISSN 11.
20. Guerhazi, E., Milano, M., Reynard, E., 2019. Performance evaluation of satellite-based rainfall products on hydrological modeling for a transboundary catchment in northwest Africa. *Theor. Appl. Climatol.* 138, 1695–1713. <https://doi.org/10.1007/s00704-019-02928-3>
21. Hua, W., Zhou, L., Nicholson, S.E., Chen, H., Qin, M., 2019. Assessing reanalysis data for understanding rainfall climatology and variability over Central Equatorial Africa. *Clim. Dyn.* 53, 651–669. <https://doi.org/10.1007/s00382-018-04604-0>
22. Huffman, G.J., Adler, R.F., Bolvin, D.T., Gu, G., Nelkin, E.J., Bowman, K.P., Hong, Y., Stocker, E.F., Wolff, D.B., 2006. The TRMM Multisatellite Precipitation Analysis (TMPA): Quasi-Global, Multiyear, Combined-Sensor Precipitation Estimates at Fine Scales. *J. Hydrometeorol.* 8, 38–55. <https://doi.org/10.1175/JHM560.1>
23. Jafarpour, M., Adib, A., Lotfirad, M., 2022. Improving the accuracy of satellite and reanalysis precipitation data by their ensemble usage. *Appl. Water Sci.* 12, 1–15. <https://doi.org/10.1007/s13201-022-01750-z>
24. Jiang, S., Zhou, M., Ren, L., Cheng, X., Zhang, P., 2016. Evaluation of latest TMPA and CMORPH satellite precipitation products over Yellow River Basin. *Water Sci. Eng.* 9, 87–96. <https://doi.org/10.1016/j.wse.2016.06.002>

25. Khan, M.K.U., Iqbal, M.F., Mahmood, I., Shahzad, M.I., Zafar, Q., Khalid, B., 2023. Evaluation of precipitation products over different climatic zones of Pakistan. *Theor. Appl. Climatol.* 151, 1301–1321. <https://doi.org/10.1007/s00704-022-04355-3>
26. Kimani, M.W., Hoedjes, J.C.B., Su, Z., 2017. An Assessment of Satellite-Derived Rainfall Products Relative to Ground Observations over East Africa. *Remote Sens.* 9. <https://doi.org/10.3390/rs9050430>
27. Liu, Z., Di, Z., Qin, P., Zhang, S., Ma, Q., 2022. Evaluation of Six Satellite Precipitation Products over the Chinese Mainland. *Remote Sens.* 14. <https://doi.org/10.3390/rs14246277>
28. Masood, M., Naveed, M., Iqbal, M., Nabi, G., Kashif, H.M., Jawad, M., Mujtaba, A., 2023. Evaluation of Satellite Precipitation Products for Estimation of Floods in Data-Scarce Environment. *Adv. Meteorol.* <https://doi.org/10.1155/2023/1685720>
29. Megersa, G., Tesfaye, K., Getnet, M., Tana, T., Jaletab, M., Lakew, B., 2019. Rainfall Variability and its Implications for Wheat and Barley Production in Central Ethiopia. *Ethiop. J. Crop Sci.* 7, 89–111.
30. Mekonen, A.A., Berlie, A.B., 2020. Spatiotemporal variability and trends of rainfall and temperature in the Northeastern Highlands of Ethiopia. *Model. Earth Syst. Environ.* 6, 285–300. <https://doi.org/10.1007/s40808-019-00678-9>
31. Miao, Y., Liu, R., Wang, Q., Jiao, L., Wang, Y., Li, L., Cao, L., 2021. Study of uncertainty of satellite and reanalysis precipitation products and their impact on hydrological simulation. *Environ. Sci. Pollut. Res.* 28, 60935–60953. <https://doi.org/10.1007/s11356-021-14847-w>
32. Moazami, S., Golian, S., Kavianpour, M.R., 2013. International Journal of Remote Comparison of PERSIANN and V7 TRMM Multi-satellite Precipitation Analysis (TMPA) products with rain gauge data over Iran. *Int. J. Remote Sens.* 34, 8156–8171. <https://doi.org/10.1080/01431161.2013.833360>
33. Park, N., Kyriakidis, P.C., Hong, S., 2017. Geostatistical Integration of Coarse Resolution Satellite Precipitation Products and Rain Gauge Data to Map Precipitation at Fine Spatial Resolutions. *Remote Sens.* 9, 1–19. <https://doi.org/10.3390/rs9030255>
34. Polong, F., Pham, Q.B., Anh, D.T., Rahman, K.U., Shahid, M., Alharbi, R.S., 2023. Evaluation and comparison of four satellite-based precipitation products over the upper Tana River Basin. *Int. J. Environ. Sci. Technol.* 20, 843–858. <https://doi.org/10.1007/s13762-022-03942-1>
35. Qi, H., 2020. Rain gauge improvement and the comprehensive effect of hydrological calculation on water resources protection. *IOP Conf. Ser. Mater. Sci. Eng.* 780, 4–8. <https://doi.org/10.1088/1757-899X/780/6/062011>
36. Qin, Y., Chen, Z., Shen, Y., Zhang, S., Shi, R., 2014. Evaluation of Satellite Rainfall Estimates over the Chinese Mainland. *Remote Sens.* 6, 11649–11672. <https://doi.org/10.3390/rs6111649>
37. Rahmawati, N., Lubczynski, M., 2018. Validation of satellite daily rainfall estimates in complex terrain of Bali Island, Indonesia. *Theor. Appl. Climatol.* 134, 513–532. <https://doi.org/10.1007/s00704-017-2290-7>
38. Seleshi, Y., Zanke, U., 2004. Recent Changes in Rainfall and Rainy Days in Ethiopia. *Int. J. Climatol.* 24, 973–983. <https://doi.org/10.1002/joc.1052>
39. Sinta, N.S., Mohammed, A.K., Ahmed, Z., Dambul, R., 2022. Evaluation of Satellite Precipitation Estimates Over Omo–Gibe River Basin in Ethiopia. *Earth Syst. Environ.* 6, 263–280. <https://doi.org/10.1007/s41748-021-00288-5>
40. Sreelash, K., Sharma, R.K., Gayathri, J.A., Upendra, B., Maya, K., Padmalal, D., 2018. Impact of Rainfall Variability on River Hydrology: A Case Study of Southern Western Ghats, India. *J. Geol. Soc. India* 92, 548–554. <https://doi.org/10.1007/s12594-018-1065-9>
41. Sutcliffe, J. V., Parks, Y.P., 1999. The hydrology of the Nile. *Hydrol. Nile. IAHS Spec. Publ. No.5.* 5.
42. Tadesse, K.E., Melesse, A.M., Abebe, A., Lakew, H.B., Paron, P., 2022. Evaluation of Global Precipitation Products over Wabi Shebelle River Basin, Ethiopia. *Hydrology* 9, 1–17. <https://doi.org/10.3390/hydrology9050066>
43. Tarek, M.H., Hassan, A., Bhattacharjee, J., Choudhury, S.H., Badruzzaman, A.B.M., 2017. Assessment of TRMM data for precipitation measurement in Bangladesh. *Meteorol. Appl.* 24, 349–359. <https://doi.org/10.1002/met.1633>

44. Thiemig, V., Rojas, R., Zambrano-Bigiarini, M., Levizzani, V., De Roo, A., 2012. Validation of satellite-based precipitation products over sparsely Gauged African River basins. *J. Hydrometeorol.* 13, 1760–1783. <https://doi.org/10.1175/JHM-D-12-032.1>
45. Wanzala, M.A., Ficchi, A., Cloke, H.L., Stephens, E.M., Badjana, H.M., Lavers, D.A., 2022. Assessment of global reanalysis precipitation for hydrological modelling in data-scarce regions: A case study of Kenya. *J. Hydrol. Reg. Stud.* 41. <https://doi.org/10.1016/j.ejrh.2022.101105>
46. Ware, M.B., Matewos, T., Guye, M., Legesse, A., Mohammed, Y., 2023. Spatiotemporal variability and trend of rainfall and temperature in Sidama Regional State, Ethiopia. *Theor. Appl. Climatol.* <https://doi.org/10.1007/s00704-023-04463-8>
47. Young, M., Williams, C., Chiu, J.C., Maidment, R., 2014. Investigation of Discrepancies in Satellite Rainfall Estimates over Ethiopia. *Am. Meteorol. Soc.* 15, 2347–2369. <https://doi.org/10.1175/JHM-D-13-0111.1>
48. Zambrano-bigiarini, M., Nauditt, A., Birkel, C., Verbist, K., Ribbe, L., 2017. Temporal and spatial evaluation of satellite-based rainfall estimates across the complex topographical and climatic gradients of Chile. *Hydrol. Earth Syst. Sci.* 21, 1295–1320. <https://doi.org/10.5194/hess-21-1295-2017>
49. Zandler, H., Haag, I., Samimi, C., 2019. Evaluation needs and temporal performance differences of gridded precipitation products in peripheral mountain regions. *Sci. Rep.* 9, 1–15. <https://doi.org/10.1038/s41598-019-51666-z>
50. Zhang, L., He, C., Tian, W., Zhu, Y., 2021. Evaluation of Precipitation Datasets from TRMM Satellite and Down-scaled Reanalysis Products with Bias-correction in Middle Qilian Mountain, China. *Chinese Geogr. Sci.* 31, 474–490. <https://doi.org/10.1007/s11769-021-1205-9>